Journal of Computational Applied Mechanics 2023, 54 (1): 127-139

DOI: 10.22059/JCAMECH.2023.354284.802

RESEARCH PAPER

Investigating the efficiency of micropiles in the stability of soil slopes: a case study

Rashid Hajivand Dastgerdi [a,], Mahmoud khalatbari [b], Abolfazl Rezaeipour [c], Alireza kiaei Fard [d], Muhammad faisal waqar [e,f], Agnieszka Malinowska [g]*

[a] *Faculty of Civil Engineering and Resource Management, AGH UST, Krakow-30065, Poland.*
[b] *Department of Mining Engineering, University of Zanjan, Zanjan, Iran.*
[c] *Asfalt Tous Company, Tehran, Iran.*
[d] *JV tractebel Consulting Company, Beirut-10999, Lebanon.*
[e] *Key Laboratory of Shale Gas and Geoengineering, Institute of Geology and Geophysics, Chinese Academy of Sciences, Beijing-100029, China.*
[f] *University of Chinese Academy of Sciences, Beijing-100049, China.*
[g] *Faculty of Mining Surveying and Environmental Engineering, AGH UST, Krakow-30065, Poland.*

Abstract

Landslides are a common geological hazard that can cause harm to human lives and property. Effective measures are necessary to prevent landslides and reduce their impact. This study investigates the effectiveness of micropiles in stabilizing a soil slope against landslides. The researchers used a computer simulation based on an example from the Plaxis software manual to model the soil slope. The simulation results showed that the safety factor, a measure of the stability of the slope, was 9% higher in the 3D model than in the 2D model when all three rows of nails were applied. In the 3D model of the soil slope, the researchers suggested using a pattern of steel pipes as micropiles to increase the safety factor of the slope and prevent landslides. It was found that a simple arrangement of steel pipes in the middle of the slope was able to stabilize the slope and result in the same level of stability as all three rows of nails. The results showed that this micropile system could be used as a low-cost and easily implementable alternative method for stabilizing soil slopes. The system is a fast and efficient way to prevent landslides, making it a potentially valuable option for those seeking to reduce the risk of landslides.

Keywords: Landslides, Micropiles, Soil Slope, Safety Factor;

1. Introduction

Landslides are coherent blocks of geo-material that slide over a failure surface, causing severe damage to natural landforms, engineering facilities, and infrastructure [1], particularly in mountainous areas. Landslides are becoming more common as extreme weather patterns and geological activities intensify. For example, between 1998 and 2017, an estimated 4.8 million people were affected by landslides, resulting in more than 18,000 deaths, with poor populations in developing or low-income countries bearing the bulk of the damage [2]. As a result, researching how to reduce the disasters caused by landslides has always been a concern for geotechnical engineers. The kinematic release of the slope, i.e., landslide, always follows a development procedure involving the formation of a shear zone

* Corresponding author. Email adress.: dastgerd@agh.edu.pl

[3-7]. Landslides must be treated quickly and effectively when disrupted traffic or operations are suspended. However, construction site spaces are typically too narrow for existing anti-sliding structures, such as large cross-section piles, retaining walls, soil nails, anchors, and so on, to be constructed on time [8, 9]. As a result, anti-sliding structures are expected to be extremely important for improving the prevention and treatment of regional landslide geological disasters, ensuring the safety of people's lives and property, and fostering harmonious social and economic development. Anti-slide piles, retaining walls, anchor cable frames, and other landslide stabilization technologies currently exist. Micropiles are a new type of anti-slide supporting structure that is popular among scholars.

Slope reinforcement measures such as anchor rod frames, retaining walls, anti-slip piles, and micropiles have all been used in construction. Among all types of reinforcement structures, micropiles are promising in engineering due to their unique performance characteristics in terms of landslide support structure lightening, miniaturization, and economic and environmental protection [10, 11]. In addition, compared to conventional anti-sliding piles, micropiles construction is relatively simple, rapid, and site flexible, with minimal disruption to slope stability, particularly for landslides in mountain areas. Micropile, also known as mini-pile, is a drilled and grouted pile with a small diameter, typically less than 300 mm, and a slenderness ratio greater than 30 [12, 13] and is made through drilling and pressure grouting. In micropiles, high-capacity body reinforcements serve as the primary load-bearing element. Steel bars, tubes, waste rails, and other materials are commonly used in these bodies. It is widely used in reinforcement engineering, particularly emergency engineering, due to the benefits of solid adaptability and fast construction [14]. Pile types can be single-row or multi-row, depending on the construction mode. Micropiles can withstand relatively large axial and moderate lateral loads and can be constructed in almost any type of soil or rock. Furthermore, micropiles are easily installed in areas with limited equipment access, such as landslides in steep, hilly, or mountainous terrain. Drilled micropiles can also be associated with other slope-stabilization techniques such as retaining walls and ground anchors. Compared to conventional large diameter bored piles [15], it has the advantages of being simpler to construct, causing less disruption to existing structures, having a higher capacity with the same volume, and having a wide range of layout options. The grouted micro-steel-pipe pile group is a common composite anti-sliding structure used for landslide stabilization in the last decade; a steel pipe with a diameter of 100-200 mm is placed in the borehole as reinforcement, and flowable grout is injected into the drilled hole at specific pressures [16]. The grout is an essential component of the micropile because it can improve the shear strength of deposits near the micropile by infiltrating into the surrounding ground via high-pressure injections; additionally, the grout can prevent corrosion of the steel pipe [17]. Micropiles in practice are connected into an integration using rigid beams or plates on top. The combination of micropiles, connecting rigid beams/plates, and surrounding rock-soil mass forms a composite structure to resist sliding thrust loads. Micropiles can be classified into two types based on their load-carrying mechanisms: (a) direct bearing and (b) reticulated root piles forming retaining walls. The reticulated root piles can resist slippage through their bottoms, providing increased stability.

Various methods have recently been used to evaluate the performance and design of micropiles used as reinforcement in slopes or landslides. Most researchers focus on their performance in stabilizing slopes under static force [18]. Recent research in China, funded by the China Geological Survey's Water and Environmental Department, used a 1:2 large-scale physical model to conduct static model testing on micropiles [19]. The models were tested and studied, including single piles, row piles, and group piles. Its verified experimentally elasticity in dynamic problems used to predict the mechanical behavior of structures [20-61]. The strength reduction method was used in this study to determine the safety factor of slopes in the finite-element procedure; the safety factors discovered were similar to those found using the limit equilibrium method for various slope angles. Furthermore, a wetting zone on the slope was found in stormy conditions, concluding that soil softening significantly influences the loss of soil cohesion. Fan and Chien [62] used a finite-element program to simulate road landslides. They studied stress distributions in reinforcements and soil nails, as well as the mechanical behavior of ecological engineering technology. Komak [63] investigated the dynamic properties of inclined micropiles to reinforce landslides using shaking table tests and discovered that inclining the micropiles reduces dynamic amplifications of acceleration on the micropiles and the soil surface.

In the present study, we investigated the efficiency of micropiles on a slope and compare their behavior with a nailing system. For this purpose, we have modeled an example from the Plaxis 2D manual, which refers to a slope stabilized with a nailing system. After modeling and validating the results of the 2D model, to increase the accuracy of the results, we converted the 2D model onto a 3D model, and all the conditions in the two-dimensional model were also considered. A comparison will be made between the results in 2D and 3D. Then, a micropile pattern was used in the 3D model to stabilize the slope instead of nails so that the efficiency of micropiles could be investigated. The safety factor will be considered the main output.

2. Case study

The case study described here concerns the construction of a new highway along the shoreline of a tidal bay on New Zealand's North Island, as shown in Figure 1[52]. The ideal location for the road would have been further away from the bay, as the slope gradients there are easier to work. However, the upper land is privately owned and cannot be altered for historical reasons, so the road must be built on a steeper gradient near the shoreline. This presents a challenge for the construction project, as the steeper slope may require additional measures to ensure the stability of the road and to protect it from tidal erosion.

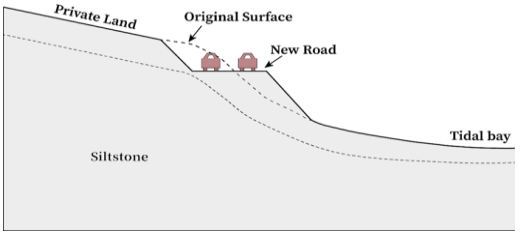

Fig 1: Situation overview for the newly constructed road

The new highway construction along the tidal bay shoreline of New Zealand's North Island is being carried out on a hillside primarily composed of siltstone. The siltstone is weathered on the surface but still solid at depth. To minimize the impact of groundwater levels, construction work is being conducted during the summer, when the water levels are low. Despite this, heavy rainfall during the winter causes the hillside almost completely to saturate. The construction process involves excavating a portion of the slope to make way for the road. The excavated material is then crushed with sand and gravel to create the road fill. Three rows of nails have been applied to the slope face to stabilize the slope. It is important to note that additional measures may be required to ensure the stability of the slope and prevent erosion, especially given the heavy rainfall during the winter months. Further information on the construction process and the stability of the slope will be discussed in subsequent sections.

3. Materials and method

This case study aims to use a slope stability example from Plaxis 2D manual to create a model and validate its results to advance the research objectives [52]. The model is depicted in Figure 2 and shows the winter groundwater level. The construction process for the new highway is outlined as follows:

- *Cutting the slope:* The slope is cut to create a wider road surface.
- *Filling in front of the slope:* The cut area is then filled with materials such as sand and gravel to widen the road surface.
- *Constructing the road:* The road is then constructed on top of the filled area.
- *Applying the nails to the soil:* Finally, nails are applied to the soil to improve the stability and safety factor of the slope.

The model in Figure 2 provides a visual representation of the construction process and the impact of the winter groundwater level on slope stability. By validating the model's results, the research can advance its goals and provide insights into the stability of the slope and the effectiveness of the construction measures taken to ensure its safety.

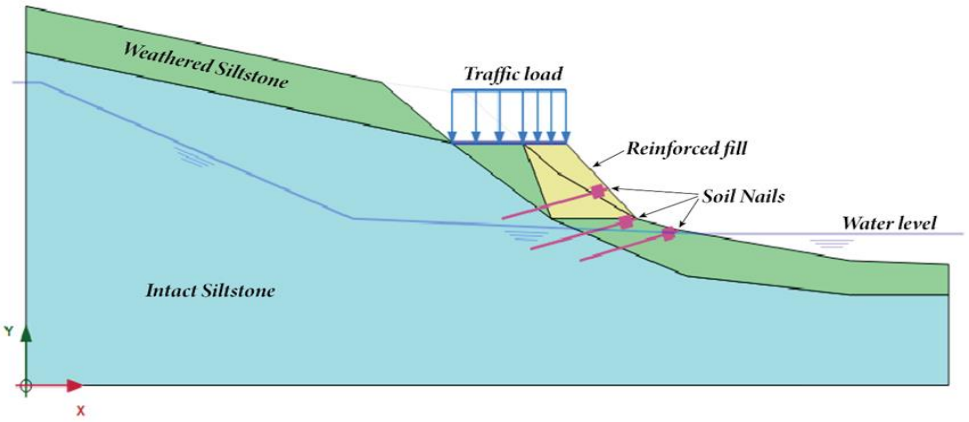

Fig 2: Plaxis 2D Model of slope stability with all components

Table 1 shows the soil properties for the area where the new highway is being constructed. The soil properties are categorized into three categories: intact siltstone, weathered siltstone, and reinforced fill. The table lists various parameters such as dry weight, wet weight, Young's modulus, Poisson's ratio, cohesion, friction angle, dilatancy angle, and permeabilities in different units. This information provides a comprehensive understanding of the soil properties and can be used to make informed decisions about the construction process and slope stability.

Table 1: Table 1: Soil properties.

Parameters	Intact siltstone	Weather siltstone	Reinforced fill	Unit
Dry weight (γ_{unsat})	16	16	19	kN/m^3
Wet weight (γ_{sat})	17	17	21	kN/m^3
Young's modulus (E')	12000	12000	20000	kN/m^2
Poisson's ratio (υ')	0.3	0.3	0.3	-
Cohesion (c'_{ref})	12	10	8	kN/m^2
Friction angle (φ')	35	19	30	°
Dilatancy angle (ψ)	0	0	0	°
Permeabilities (k_x, k_y)	1×10^{-3}	0.01	0.1	m/d

Table 2 lists the properties of the road surface used in the model. A plate element has been used to represent the road surface. The parameters listed in the table include axial stiffness (EA_1, EA_2), flexural stiffness (EI), weight (w), and Poisson's ratio (υ). Axial stiffness (EA_1, EA_2) refers to the stiffness of the road surface in the axial direction and is given in units of kN/m. Flexural stiffness (EI) is a measure of the road's resistance to bending and is given in units of $kN.m^2/m$. Weight (w) represents the weight of the road surface and is given in units of kNm/m. Poisson's ratio (v) describes the relationship between the road's lateral and axial strains and is set to 0.0 in this model. This information is essential in determining the overall stability and performance of the road surface.

Table 2: Properties of the road surface.

Parameters	Road surface	Unit
Axial stiffness (EA_1, EA_2)	2.5×10^5	kN/m
Flexural stiffness (EI)	500	$kN.m^2/m$
Weight (w)	3	kNm/m
Poisson's ratio (υ)	0.0	-

Table 3 describes the properties of the soil nails used in the model. The nails have been modeled as embedded beam row elements. The parameters listed in the table include modulus of elasticity (E), material weight (γ), diameter, spacing ($L_{spacing}$), and skin resistance ($T_{skin,start,max}$, $T_{skin,end,max}$). The modulus of elasticity (E) is a measure of the stiffness of the nails and is given in units of kN/m^2. Material weight (γ) is the weight of the nails per unit area and is given in units of kN/m^2. Diameter refers to the size of the nails and is given in units of meters. Spacing

($L_{spacing}$) refers to the distance between nails and is given in units of meters. Skin resistance ($T_{skin,start,max}$, $T_{skin,end,max}$) represents the maximum tension that can be developed in the nails and is given in units of kN/m. These properties of the soil nails are important in understanding their contribution to the overall stability of the slope.

Table 3: Properties of the soil nails (embedded beam row).

Parameters	Grout body	Unit
Modulus of elasticity (E)	210×10^6	kN/m^2
Material weight (γ)	60	kN/m^2
Diameter	0.032	m
Spacing ($L_{spacing}$)	1.0	m
Skin resistance ($T_{skin,start,max}$, $T_{skin,end,max}$)	1000	kN/m

In this case study, the safety factor for each construction phase was calculated using Plaxis 2D manual. The calculation results showed the safety factors under different conditions, represented in Figure 3. The conditions included the groundwater level in winter and summer, where in summer the groundwater level is equal to the ocean water level, and in winter it is higher due to increased atmospheric precipitation. The results of the safety factor calculation provide insight into the stability of the slope during construction and can be used to advance the research goals.

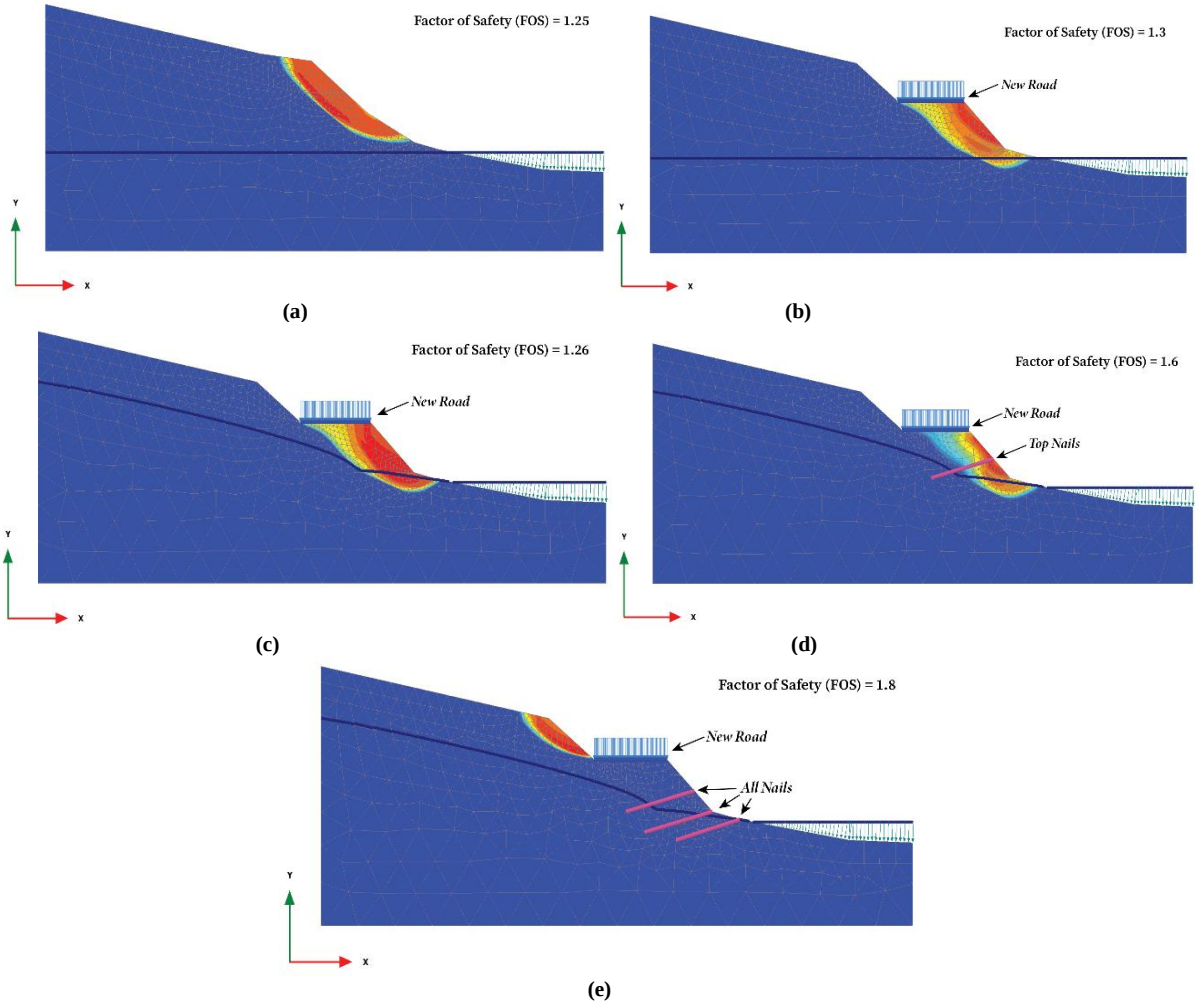

Fig 2: Critical zone of the 2D model at different conditions (a) Before constructing the road during summer (b) After constructing the road during summer (c) After constructing the road during winter (d) after applying top nails during winter (e) after applying all nails during winter

In figure 4, the results of the safety factors for the slope are displayed in a graph to compare the values under different conditions. The natural ground surface has a safety factor of 1.25 during the summer, which increases to 1.3 after construction due to the excavation and embankment. However, the safety factor decreases to 1.25 during winter due to the increased groundwater levels. To address this, the engineers applied one row of nails with 1 meter spacing on the upper side of the embankment. Subsequently, they applied three rows of nails with a spacing of 1 meter on the embankment, which increased the final safety factor from 1.6 (with one row of nails) to 1.8 (with three rows of nails). The results obtained from the built model agree with the manual results from Plaxis.

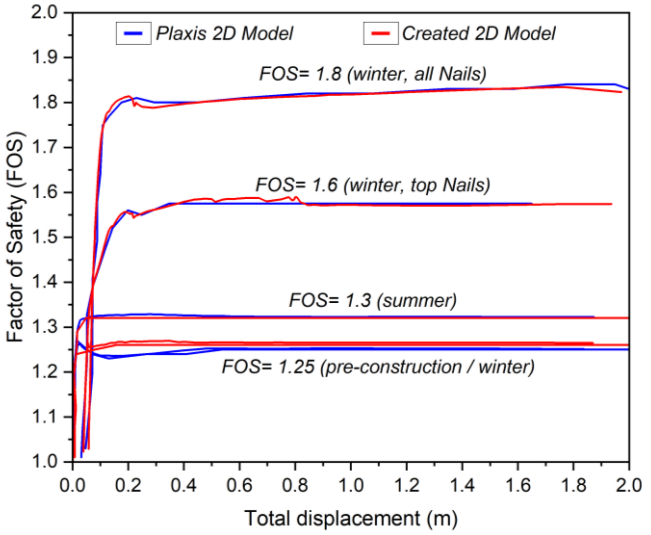

Fig 4: Comparing FOS for created 2d model versus Plaxis 2d manual model

4. Three-Dimensional Modelling

The research conduct aimed to understand the behavior of nails and micropiles in the slope stability model. To do so, they first assessed the impact of using a 3D modeling approach instead of the 2D modeling approach used in the Plaxis software manual. The 2D model was based on the assumption of plane strain, which is a simplification that reduces calculation time but is not suitable for modeling structural elements that are separate and non-continuous. In recent years, the Plaxis 2D software has added new tools to mitigate this problem, but the researchers still decided to create a 3D model for increased accuracy. The 3D model was created by keeping the same geometry as the 2D model and adding a depth of 10 m in the Y direction. The conditions in the 3D model were the same as those in the 2D model, but the researchers used an embedded beam element to simulate the nails and the micropiles. In this particular section, only the nails were modeled, and the behavior of the slope with a single nail row was not considered. The results of the 3D model showed close agreement with the 2D analysis results, as evidenced by the critical zones obtained from both models. The location of these critical zones was found to be in close agreement between the two models (as shown in Figure 5). This highlights the importance of using a 3D modeling approach when modeling the behavior of structural elements such as nails and micropiles in slope stability.

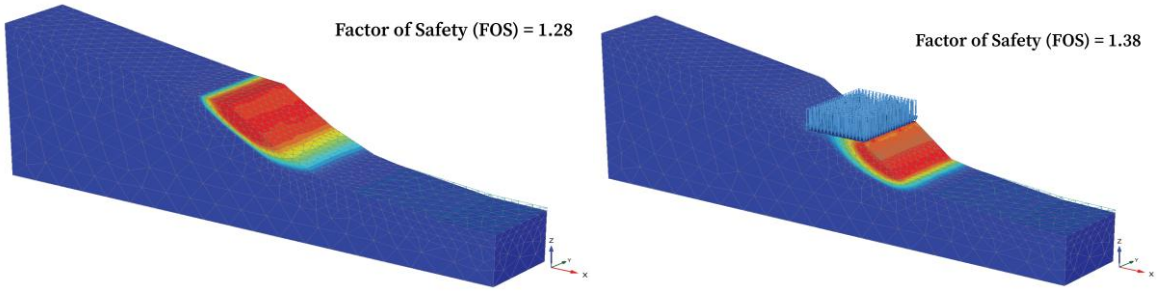

(a) **(b)**

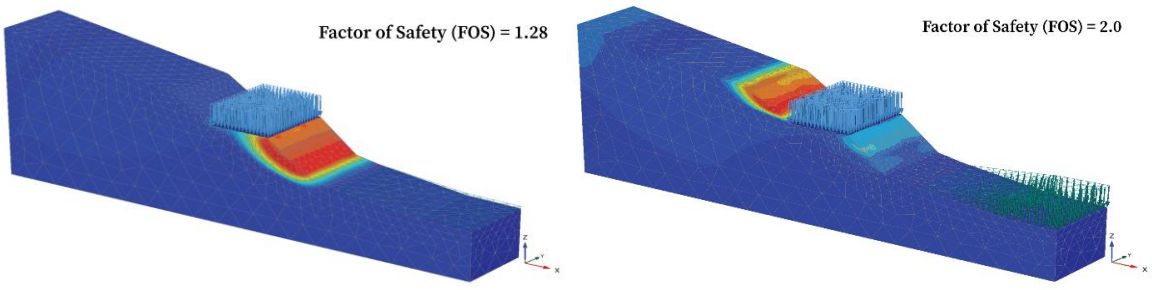

Fig. 5: Critical zone of the 3D model at different conditions (a) Pre-construction during summer (b) After constructing the road during summer (c) After constructing the road during winter (d) after applying all nails during winter

Figure 6 presents the results of a comparison between the safety factors calculated from 2D and 3D models. It is common to observe that the safety factor calculated from a 3D model is slightly higher compared to that calculated from a 2D model. This is due to the fact that 3D models provide a more realistic representation of the conditions and behavior of the structure being analyzed. The graph shows that the safety factor for the natural surface calculated from both 2D and 3D models is the almost same before construction. The same is true for the safety factor calculated during the summer after construction and for the construction during winter without nails. However, after applying all nails during the winter, there is a 10% difference between the safety factor calculated from the 2D and 3D models. This difference highlights the importance of using 3D models to get a more accurate and realistic representation of the safety of the analyzed structure.

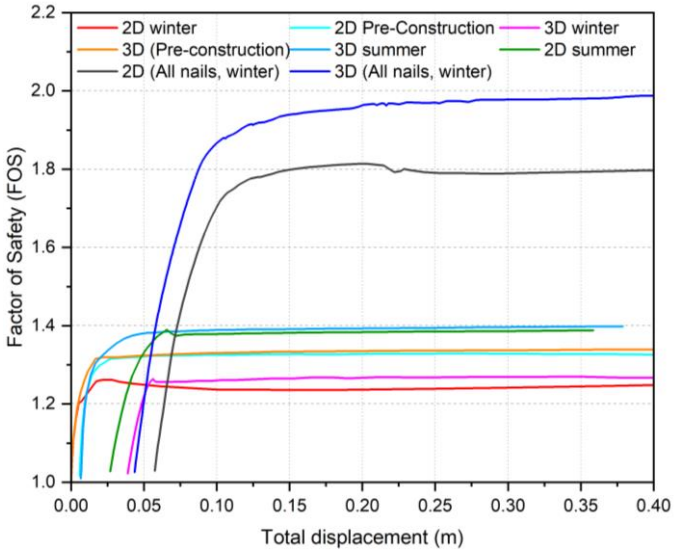

Fig. 6: Comparison the safety factor of 2D and 3D models

5. Micro pile reinforcement

Micropiles are cylindrical elements with a diameter ranging from 10 to 30 cm and are used to bear axial loads. They are used in a variety of ways such as in a single, group, or network pattern. In recent years, micropiles have become popular for slope stability projects as they offer several advantages. Firstly, they are simple to construct and have a quick implementation time. Secondly, they do not require heavy or special equipment, which leads to lower construction costs. Thirdly, micropiles increase the stability of the slopes by counteracting the shear force mobilized in the soil, which helps to prevent its horizontal movement. Overall, micropiles are an effective solution for slope stability projects due to their ease of construction, quick implementation, and cost-effectiveness. Nails are commonly used to strengthen the stability of slopes for faster implementation and a reduced final cost, although micropiles can also be employed for the same purposes. The current study was carried out to elucidate the application of micropiles in slope stability. As a result, instead of nails, we used two rows of micropiles spaced 1 m apart in the centre of the slope in the 3D model. We used 6 m long pipes with a thickness of 6 mm for micropiles inserted in the soil after drilling. Gravity also injects concrete into the pipelines, and a uniform concrete cap 40 x 40 cm in size was utilized

on top of the micropiles for integrity. The micropiles are modeled using the embedded beam element. The characteristics of the micropiles are listed in Table 4.

Table 4: Micro pile properties used in the study.

Diameter (D)	Thickness	Micropile Spacing	Modulus of elasticity (E)	Material Weight (γ)	Axial skin resistance	Base resistance
0.15	0.006	1	210×10^6	78	Layer dependent	0
m	m	m	kN/m^2	kN/m^3	-	kN/m^2

The figure 7 shows the placement and arrangement of the micropiles in the model. The illustration shows how the micropiles are positioned within the slope. It is important to mention that the pattern illustrated in the figure gives the best results in terms of preventing soil movements and increasing the safety factor with the same materials. The micropiles are placed in two rows with a spacing of 1 meter in the middle of the slope to provide stability to the soil and prevent soil movement. The use of micropiles in slope stability projects provides advantages such as increasing safety factors with the same materials, and no need for heavy and special equipment.

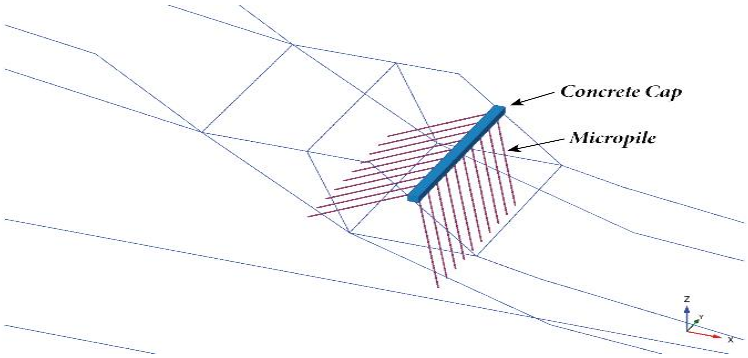

Fig. 7: location and pattern of micropiles constructed on slope

Figure 8 shows the critical zone of the slope stability model that has been reinforced with micropiles. The figure illustrates the area of the model with the lowest safety factor. It can be observed that the micropiles have effectively prevented the horizontal movement of the soil mass and have stabilized the soil in the embankment area. Despite the success of the micropiles in stabilizing the soil, it can also be seen that the soil above the road remains the second most critical part of the model, just as it was in the unreinforced model. The figure demonstrates that the micropiles have successfully increased the slope's stability, but the soil above the road still requires further reinforcement.

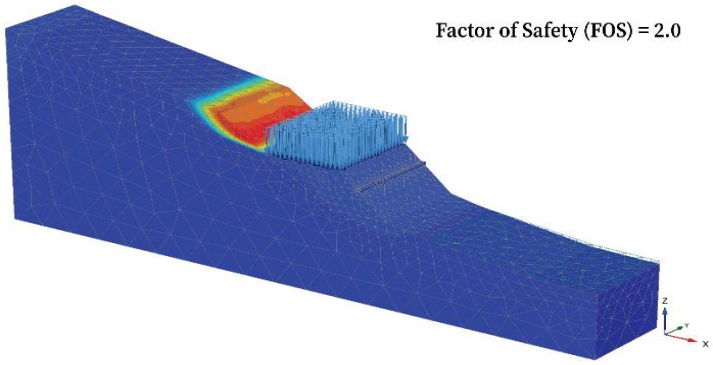

Fig. 8: critical zone of the model after applying micropiles to the slope in 3D model, during winter

Figure 9 provides a comparison of the safety factor values of the models with both nails and micropiles during winter conditions. The graph presents two curves, one for each type of reinforcement. The curves show the safety factor for the soil above the road, which was found to be the most critical zone in the previous analysis. The graph clearly indicates that after the reinforcement with micropiles, the safety factor value has increased significantly as compared to the model with nails. However, the soil above the road remains the critical zone with the lowest safety

factor, with a value of around 2. This suggests that while micropiles have increased the soil mass's stability, further reinforcements may be required to completely stabilize the slope.

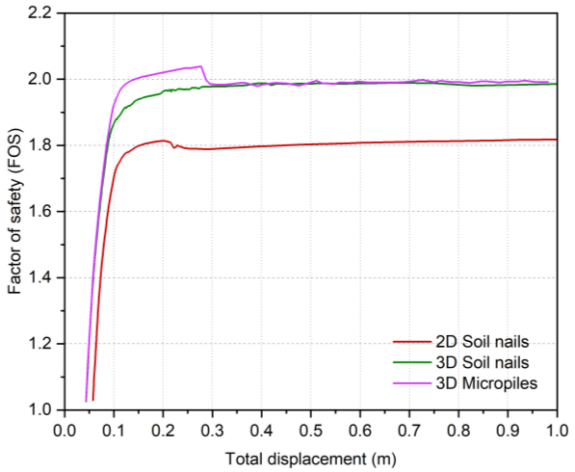

Fig. 9: Comparison the safety factor of 2D, 3D models of soil nails and micropiles

The safety factor for the entire model, including the soil above the road and the embankment, is calculated by the Plaxis software. The researchers adjusted the cohesion and internal friction angle of the soil above the road to precisely compute the safety factor for the embankment as the second important location. To determine the safety factor, the Plaxis software use the C/Phi reduction approach. Figures 10 and 11 show the critical zone and safety factor for the main slope (embankment) after three rows of nails and micropiles were installed during the winter. The figures reveal that the nails and micropiles effectively stabilized the soil in the embankment area, which is the model's second critical zone.

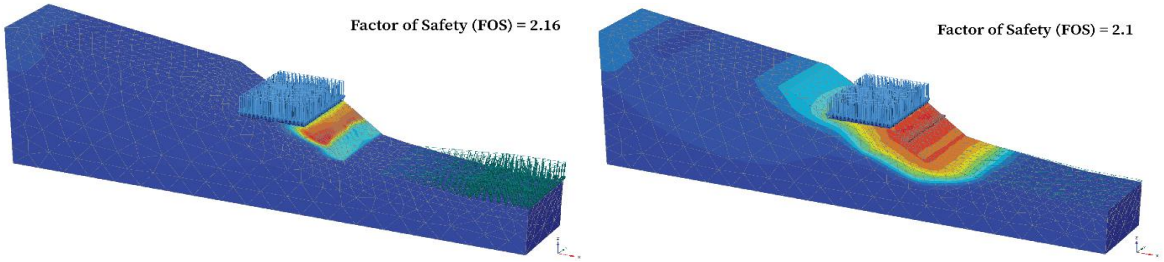

Fig. 10: Critical zone and safety factor for both models reinforced with three row of nails and micropiles

The study concluded that both the nailing and micropile methods can effectively stabilize the road slope, resulting in an almost equal safety factor of 2.1, which is deemed sufficient for a road slope. The use of micropiles with the specific pattern demonstrated in the research can be an alternative option for slope stabilization compared to the traditional nailing method.

6. Conclusion

The following conclusions are made from the study:

- The study focuses on evaluating the performance of micropiles in slope stability. The research uses a 2D model from the Plaxis software manual as the base model and validates the results. The 2D model is then converted into a 3D model, and it is observed that the safety factor of the slope during winter when nails are applied in the 3D model is 10% higher compared to the 2D model.
- The use of 3D modeling was preferred as it provides more realistic results. To evaluate the performance of micropiles, two inclined rows of steel pipes filled with concrete were used. The type and arrangement of micropiles were selected in such a way as to increase the safety factor of the slope, as is done when

using nails for stabilization. The micropiles used in the study had 6 m length, 15 cm diameter, and 6 mm thickness.

- The critical zone and safety factor results show that the presented micro pile system can be used as an alternative method to stabilize slopes. The method is low-cost, fast to construct, and easy to implement.

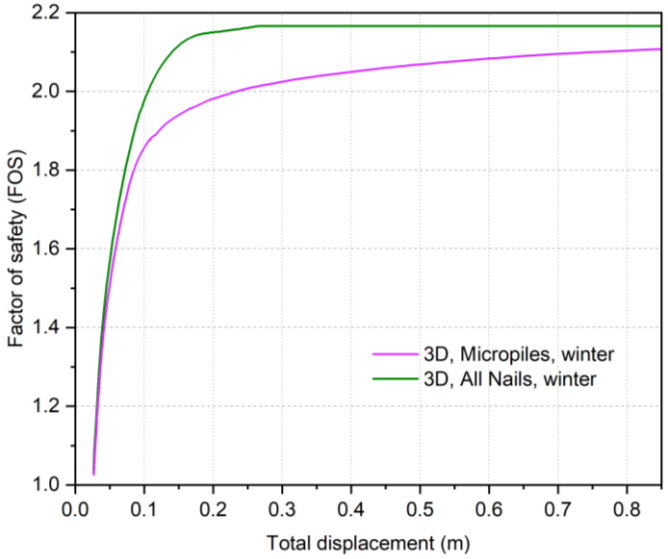

Fig. 11: Comparison the safety factor of the main slope after applying nails and micropiles

7. Nomenclature

2D	Two-dimensional
3D	Three-dimensional
FOS	Factor of safety
γ_{unsat}	Dry weight
γ_{sat}	Wet weight
E'	Effective young's modulus
υ'	Effective poisson's ratio
c'_{ref}	Effective cohesion
φ'	Effective friction angle
ψ	Dilatancy angle
k_x, k_y	Permeabilities
EA_1, EA_2	Axial stiffness
EI	Flexural stiffness
w	Weight
υ	Poisson's ratio
E	Modulus of elasticity
γ	Material weight
$L_{spacing}$	Spacing
T_{skin}	Skin resistance

References

[1] S.-W. Sun, F.-Q. Chen, W. Wang, Mechanism and remediation of a seismically induced landslide with a potential for deep seated sliding, *Soil Mechanics and Foundation Engineering*, Vol. 52, No. 3, pp. 155-162, 2015.

[2] P. Wallemacq, R. Below, D. McClean, 2018, *Economic losses, poverty & disasters: 1998-2017*, United Nations Office for Disaster Risk Reduction,

[3] S. Guo, S. Qi, Numerical study on progressive failure of hard rock samples with an unfilled undulate joint, *Engineering Geology*, Vol. 193, pp. 173-182, 2015.

[4] S. Guo, S. Qi, Z. Zhan, L. Ma, E. G. Gure, S. Zhang, Numerical study on the progressive failure of heterogeneous geomaterials under varied confining stresses, *Engineering Geology*, Vol. 269, pp. 105556, 2020.

[5] S. Guo, S. Qi, G. Yang, S. Zhang, C. Saroglou, An analytical solution for block toppling failure of rock slopes during an earthquake, *Applied Sciences*, Vol. 7, No. 10, pp. 1008, 2017.

[6] S. Guo, S. Qi, Y. Zou, B. Zheng, Numerical studies on the failure process of heterogeneous brittle rocks or rock-like materials under uniaxial compression, *Materials*, Vol. 10, No. 4, pp. 378, 2017.

[7] S. Guo, S. Qi, Z. Zhan, B. Zheng, Plastic-strain-dependent strength model to simulate the cracking process of brittle rocks with an existing non-persistent joint, *Engineering Geology*, Vol. 231, pp. 114-125, 2017.

[8] B. Xu, Landslide Control and Analysis, Beijing: China Railway Publishing House, 2001.

[9] Z. Chen, Z. Wang, H. Xi, Z. Yang, L. Zou, Z. Zhou, C. Zhou, Recent advances in high slope reinforcement in China: Case studies, *Journal of Rock Mechanics and Geotechnical Engineering*, Vol. 8, No. 6, pp. 775-788, 2016.

[10] K. T. Chau, C. Shen, X. Guo, Nonlinear seismic soil–pile–structure interactions: shaking table tests and FEM analyses, *Soil Dynamics and Earthquake Engineering*, Vol. 29, No. 2, pp. 300-310, 2009.

[11] Y. Mascarucci, S. Miliziano, A. Mandolini, A numerical approach to estimate shaft friction of bored piles in sands, *Acta Geotechnica*, Vol. 9, pp. 547-560, 2014.

[12] D. Bruce, I. Juran, Drilled and Grouted Micropiles: State-of-Practice Review, Volume I: Background, Classifications, Cost, 1997.

[13] S. Xiao, K. Cui, D. Zhou, J. Feng, *Analysis of a new combined micropile structure for preventing slope slippage and its application in a practical project*, in: *ICCTP 2009: Critical Issues In Transportation Systems Planning, Development, and Management*, Eds., pp. 1-11, 2009.

[14] G. Ghataora, L. Lee, U. Ling, Changes in properties of clay surrounding cast in situ piles, *Geotechnical and Geological Engineering*, Vol. 29, pp. 57-63, 2011.

[15] C.-G. Qi, G.-B. Liu, Y. Wang, Y.-B. Deng, A design method for plastic tube cast-in-place concrete pile considering cavity contraction and its validation, *Computers and Geotechnics*, Vol. 69, pp. 262-271, 2015.

[16] B. Xiang, L. Zhang, L.-R. Zhou, Y.-Y. He, L. Zhu, Field lateral load tests on slope-stabilization grouted pipe pile groups, *Journal of Geotechnical and Geoenvironmental Engineering*, Vol. 141, No. 4, pp. 04014124, 2015.

[17] M. Aboutabikh, A. Soliman, M. El Naggar, Performance of hollow bar micropiles using green grout incorporating treated oil sand waste, *Journal of Building Engineering*, Vol. 27, pp. 100964, 2020.

[18] H. Bayesteh, M. A. Fakharnia, M. Khodaparast, Performance of driven grouted micropiles: full-scale field study, *International Journal of Geomechanics*, Vol. 21, No. 2, pp. 04020250, 2021.

[19] J. Wang, J. Zhang, Preliminary engineering application of microseismic monitoring technique to rockburst prediction in tunneling of Jinping II project, *Journal of Rock Mechanics and Geotechnical Engineering*, Vol. 2, No. 3, pp. 193-208, 2010.

[20] M. Mohammadi, A. Farajpour, A. Moradi, M. Hosseini, Vibration analysis of the rotating multilayer piezoelectric Timoshenko nanobeam, *Engineering Analysis with Boundary Elements*, Vol. 145, pp. 117-131, 2022.

[21] M. Mohammadi, A. Rastgoo, Primary and secondary resonance analysis of FG/lipid nanoplate with considering porosity distribution based on a nonlinear elastic medium, *Mechanics of Advanced Materials and Structures*, Vol. 27, No. 20, pp. 1709-1730, 2020.

[22] M. Mohammadi, M. Hosseini, M. Shishesaz, A. Hadi, A. Rastgoo, Primary and secondary resonance analysis of porous functionally graded nanobeam resting on a nonlinear foundation subjected to mechanical and electrical loads, *European Journal of Mechanics-A/Solids*, Vol. 77, pp. 103793, 2019.

[23] M. Mohammadi, A. Rastgoo, Nonlinear vibration analysis of the viscoelastic composite nanoplate with three directionally imperfect porous FG core, *Structural Engineering and Mechanics, An Int'l Journal*, Vol. 69, No. 2, pp. 131-143, 2019.

[24] A. Farajpour, A. Rastgoo, M. Mohammadi, Vibration, buckling and smart control of microtubules using piezoelectric nanoshells under electric voltage in thermal environment, *Physica B: Condensed Matter*, Vol. 509, pp. 100-114, 2017.

[25] A. Farajpour, M. H. Yazdi, A. Rastgoo, M. Loghmani, M. Mohammadi, Nonlocal nonlinear plate model for large amplitude vibration of magneto-electro-elastic nanoplates, *Composite Structures*, Vol. 140, pp. 323-336, 2016.

[26] A. Farajpour, M. H. Yazdi, A. Rastgoo, M. Mohammadi, A higher-order nonlocal strain gradient plate model for buckling of orthotropic nanoplates in thermal environment, *Acta Mechanica,* Vol. 227, pp. 1849-1867, 2016.

[27] M. Mohammadi, M. Safarabadi, A. Rastgoo, A. Farajpour, Hygro-mechanical vibration analysis of a rotating viscoelastic nanobeam embedded in a visco-Pasternak elastic medium and in a nonlinear thermal environment, *Acta Mechanica,* Vol. 227, pp. 2207-2232, 2016.

[28] M. R. Farajpour, A. Rastgoo, A. Farajpour, M. Mohammadi, Vibration of piezoelectric nanofilm-based electromechanical sensors via higher-order non-local strain gradient theory, *Micro & Nano Letters,* Vol. 11, No. 6, pp. 302-307, 2016.

[29] M. Baghani, M. Mohammadi, A. Farajpour, Dynamic and stability analysis of the rotating nanobeam in a nonuniform magnetic field considering the surface energy, *International Journal of Applied Mechanics,* Vol. 8, No. 04, pp. 1650048, 2016.

[30] M. Goodarzi, M. Mohammadi, M. Khooran, F. Saadi, Thermo-mechanical vibration analysis of FG circular and annular nanoplate based on the visco-pasternak foundation, *Journal of Solid Mechanics,* Vol. 8, No. 4, pp. 788-805, 2016.

[31] H. Asemi, S. Asemi, A. Farajpour, M. Mohammadi, Nanoscale mass detection based on vibrating piezoelectric ultrathin films under thermo-electro-mechanical loads, *Physica E: Low-dimensional Systems and Nanostructures,* Vol. 68, pp. 112-122, 2015.

[32] M. Safarabadi, M. Mohammadi, A. Farajpour, M. Goodarzi, Effect of surface energy on the vibration analysis of rotating nanobeam, 2015.

[33] M. Goodarzi, M. Mohammadi, A. Gharib, Techno-Economic Analysis of Solar Energy for Cathodic Protection of Oil and Gas Buried Pipelines in Southwestern of Iran, in *Proceeding of,* https://publications.waset.org/abstracts/33008/techno-economic-analysis-of …, pp.

[34] M. Mohammadi, A. A. Nekounam, M. Amiri, The vibration analysis of the composite natural gas pipelines in the nonlinear thermal and humidity environment, in *Proceeding of,* https://civilica.com/doc/540946/, pp.

[35] M. Goodarzi, M. Mohammadi, M. Rezaee, Technical Feasibility Analysis of PV Water Pumping System in Khuzestan Province-Iran, in *Proceeding of,* https://publications.waset.org/abstracts/18930/technical-feasibility …, pp.

[36] M. Mohammadi, A. Farajpour, A. Moradi, M. Ghayour, Shear buckling of orthotropic rectangular graphene sheet embedded in an elastic medium in thermal environment, *Composites Part B: Engineering,* Vol. 56, pp. 629-637, 2014.

[37] M. Mohammadi, A. Moradi, M. Ghayour, A. Farajpour, Exact solution for thermo-mechanical vibration of orthotropic mono-layer graphene sheet embedded in an elastic medium, *Latin American Journal of Solids and Structures,* Vol. 11, pp. 437-458, 2014.

[38] M. Mohammadi, A. Farajpour, M. Goodarzi, F. Dinari, Thermo-mechanical vibration analysis of annular and circular graphene sheet embedded in an elastic medium, *Latin American Journal of Solids and Structures,* Vol. 11, pp. 659-682, 2014.

[39] M. Mohammadi, A. Farajpour, M. Goodarzi, Numerical study of the effect of shear in-plane load on the vibration analysis of graphene sheet embedded in an elastic medium, *Computational Materials Science,* Vol. 82, pp. 510-520, 2014.

[40] A. Farajpour, A. Rastgoo, M. Mohammadi, Surface effects on the mechanical characteristics of microtubule networks in living cells, *Mechanics Research Communications,* Vol. 57, pp. 18-26, 2014.

[41] S. R. Asemi, M. Mohammadi, A. Farajpour, A study on the nonlinear stability of orthotropic single-layered graphene sheet based on nonlocal elasticity theory, *Latin American Journal of Solids and Structures,* Vol. 11, pp. 1541-1546, 2014.

[42] M. Goodarzi, M. Mohammadi, A. Farajpour, M. Khooran, Investigation of the effect of pre-stressed on vibration frequency of rectangular nanoplate based on a visco-Pasternak foundation, 2014.

[43] S. Asemi, A. Farajpour, H. Asemi, M. Mohammadi, Influence of initial stress on the vibration of double-piezoelectric-nanoplate systems with various boundary conditions using DQM, *Physica E: Low-dimensional Systems and Nanostructures,* Vol. 63, pp. 169-179, 2014.

[44] S. Asemi, A. Farajpour, M. Mohammadi, Nonlinear vibration analysis of piezoelectric nanoelectromechanical resonators based on nonlocal elasticity theory, *Composite Structures,* Vol. 116, pp. 703-712, 2014.

[45] M. Mohammadi, M. Ghayour, A. Farajpour, Free transverse vibration analysis of circular and annular graphene sheets with various boundary conditions using the nonlocal continuum plate model, *Composites Part B: Engineering,* Vol. 45, No. 1, pp. 32-42, 2013.

[46] M. Mohammadi, M. Goodarzi, M. Ghayour, A. Farajpour, Influence of in-plane pre-load on the vibration frequency of circular graphene sheet via nonlocal continuum theory, *Composites Part B: Engineering*, Vol. 51, pp. 121-129, 2013.

[47] M. Mohammadi, A. Farajpour, M. Goodarzi, R. Heydarshenas, Levy type solution for nonlocal thermo-mechanical vibration of orthotropic mono-layer graphene sheet embedded in an elastic medium, *Journal of Solid Mechanics*, Vol. 5, No. 2, pp. 116-132, 2013.

[48] M. Mohammadi, A. Farajpour, M. Goodarzi, H. Mohammadi, Temperature Effect on Vibration Analysis of Annular Graphene Sheet Embedded on Visco-Pasternak Foundati, *Journal of Solid Mechanics*, Vol. 5, No. 3, pp. 305-323, 2013.

[49] S. Ghannadpour, B. Mohammadi, J. Fazilati, Bending, buckling and vibration problems of nonlocal Euler beams using Ritz method, *Composite Structures*, Vol. 96, pp. 584-589, 2013.

[50] M. Danesh, A. Farajpour, M. Mohammadi, Axial vibration analysis of a tapered nanorod based on nonlocal elasticity theory and differential quadrature method, *Mechanics Research Communications*, Vol. 39, No. 1, pp. 23-27, 2012.

[51] A. Farajpour, A. Shahidi, M. Mohammadi, M. Mahzoon, Buckling of orthotropic micro/nanoscale plates under linearly varying in-plane load via nonlocal continuum mechanics, *Composite Structures*, Vol. 94, No. 5, pp. 1605-1615, 2012.

[52] M. Mohammadi, M. Goodarzi, M. Ghayour, S. Alivand, Small scale effect on the vibration of orthotropic plates embedded in an elastic medium and under biaxial in-plane pre-load via nonlocal elasticity theory, 2012.

[53] A. Farajpour, M. Mohammadi, A. Shahidi, M. Mahzoon, Axisymmetric buckling of the circular graphene sheets with the nonlocal continuum plate model, *Physica E: Low-dimensional Systems and Nanostructures*, Vol. 43, No. 10, pp. 1820-1825, 2011.

[54] A. Farajpour, M. Danesh, M. Mohammadi, Buckling analysis of variable thickness nanoplates using nonlocal continuum mechanics, *Physica E: Low-dimensional Systems and Nanostructures*, Vol. 44, No. 3, pp. 719-727, 2011.

[55] H. Moosavi, M. Mohammadi, A. Farajpour, S. Shahidi, Vibration analysis of nanorings using nonlocal continuum mechanics and shear deformable ring theory, *Physica E: Low-dimensional Systems and Nanostructures*, Vol. 44, No. 1, pp. 135-140, 2011.

[56] M. Mohammadi, M. Ghayour, A. Farajpour, Analysis of free vibration sector plate based on elastic medium by using new version differential quadrature method, *Journal of solid mechanics in engineering*, Vol. 3, No. 2, pp. 47-56, 2011.

[57] A. Farajpour, M. Mohammadi, M. Ghayour, Shear buckling of rectangular nanoplates embedded in elastic medium based on nonlocal elasticity theory, in *Proceeding of*, www.civilica.com/Paper-ISME19-ISME19_390.html, pp. 390.

[58] M. Mohammadi, A. Farajpour, A. R. Shahidi, Higher order shear deformation theory for the buckling of orthotropic rectangular nanoplates using nonlocal elasticity, in *Proceeding of*, www.civilica.com/Paper-ISME19-ISME19_391.html, pp. 391.

[59] M. Mohammadi, A. Farajpour, A. R. Shahidi, Effects of boundary conditions on the buckling of single-layered graphene sheets based on nonlocal elasticity, in *Proceeding of*, www.civilica.com/Paper-ISME19-ISME19_382.html, pp. 382.

[60] M. Mohammadi, M. Ghayour, A. Farajpour, Using of new version integral differential method to analysis of free vibration orthotropic sector plate based on elastic medium, in *Proceeding of*, www.civilica.com/Paper-ISME19-ISME19_497.html, pp. 497.

[61] M. Mohammadi, A. Farajpour, A. Rastgoo, Coriolis effects on the thermo-mechanical vibration analysis of the rotating multilayer piezoelectric nanobeam, *Acta Mechanica*, Vol. 234, No. 2, pp. 751-774, 2023/02/01, 2023.

[62] C. Fan, Application of finite element procedures on the slope stability analysis in stormy condition, *Sino-Geotech*, Vol. 95, pp. 61-74, 2003.

[63] A. Komak Panah, H. Jalilian Mashhoud, J.-H. Yin, Y. Fai Leung, Shaking table investigation of effects of inclination angle on seismic performance of micropiles, *International Journal of Geomechanics*, Vol. 18, No. 11, pp. 04018142, 2018.